A Comprehensive Study on Equivalent Modulation Waveforms of the SVM Sequence for Three-Level Inverters

Juan Chen, Yingjie He, *Member, IEEE*, Saad Ul Hasan, *Member, IEEE*, and Jinjun Liu, *Senior Member, IEEE*

***Abstract*—According to the number of segments, the space vector modulation (SVM) can divide into conventional SVM sequence (CSVMS) and special SVM sequence (SSVMS). It is well known that SVM can be equivalently realized by carrier-based pulse width modulation (CBPWM) with a zero component injection in both two-level and three-level inverters. For eight segment CSVMS in three-level inverters, many papers have ever got the injected zero component equation. But similar approach does not work for SSVMS, which has more than eight segments, e.g., 10, 12, or 14. What more, the accurate injected zero component has never been achieved so far. To solve above problems, therefore, a generated decomposition method of modulation wave has been proposed in this paper. By strict theoretical derivation, the same correlation can be extended to SSVMS and the corresponding zero component expression can be acquired. Based on this method, this paper puts a lot attention on the essential feature explanation, mathematical proof, and gives a detailed process to get the zero component equation, using it can realize SSVMS by CBPWM. The simulation and experimental results illustrate that the generated decomposition method of modulation wave is correct, and the unified theory of CBPWM and SVM is verified.**

***Index Terms*—Carrier-based pulse width modulation (CBPWM), inherent correlation, space vector modulation (SVM), three-level voltage source inverter.**

I. Introduction

AMONG numerous pulse width modulation (PWM) techniques, carrier-based pulse width modulation (CBPWM) and space vector modulation (SVM) are the most popular modulators. It is well recognized that SVM can function equivalently to CBPWM by adding zero-sequence component or common-mode injections in two-level inverters [1]–[4] and three-level or even multilevel inverters [5]–[7]. Compared to CBPWM, SVM has several benefits, such as producing the highest available fundamental output voltage, low-harmonic distortion in the output current, and suitable for digital implementation. It also can be used for balancing dc neutral point by chosing the proper redundant vectors, but SVM will be very complicated when applied to three or more high-level inverters. By injecting the zero-sequence component, superior performance such as the neutral point voltage balance, switching frequency reduction, switching losses, and the linear modulation range can be achieved by

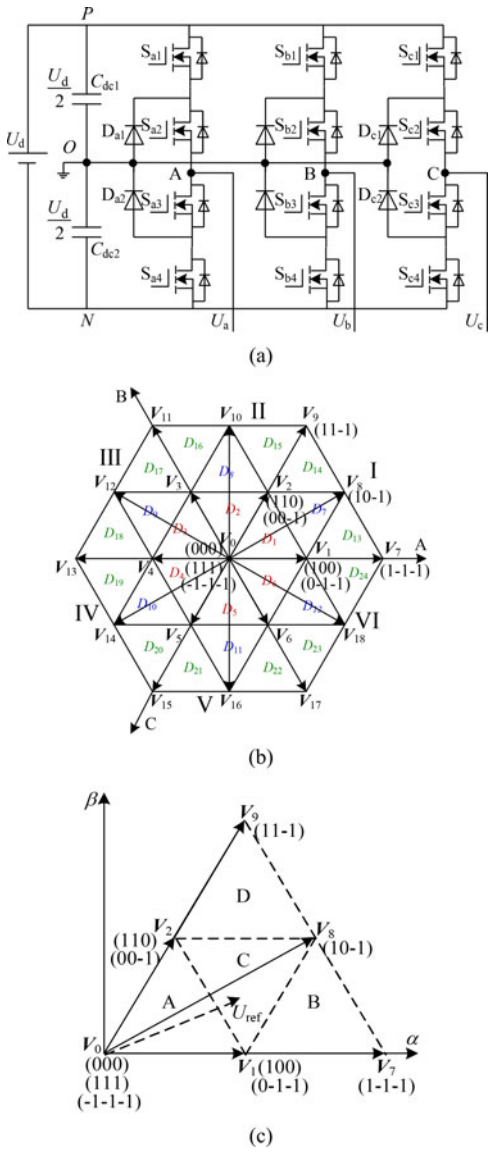

Fig. 1. (a) Main circuit of three-level NPC inverter. (b) Space vector diagram of three-level NPC VSI. (c) Space vector diagram of Sector I.

Manuscript received July 27, 2014; revised December 3, 2014 and October 7, 2014; accepted December 29, 2014. Date of publication January 12, 2015; date of current version August 21, 2015. This work was supported in part by the National Natural Science Foundation of China (50907052), by the Shaanxi Natural Science Fund (2014JQ7271), by the Innovation Fund of Status Key Laboratory of Electrical Insulation and Power Equipment (EIPE13307), and by the Delta Educational Development Foundation (DREG2013007). Recommended for publication by Associate Editor A. M. Trzynadlowski.

The authors are with the State Key Lab of Electrical Insulation and Power Equipment, School of Electrical Engineering, Xi'an Jiaotong University, Xi'an 710049, China (e-mail: cj_star@qq.com; hyj202411@sina.com; saad_barlas@hotmail.com; jjliu@xjtu.edu.cn).

Color versions of one or more of the figures in this paper are available online at http://ieeexplore.ieee.org.

Digital Object Identifier 10.1109/TPEL.2015.2391096

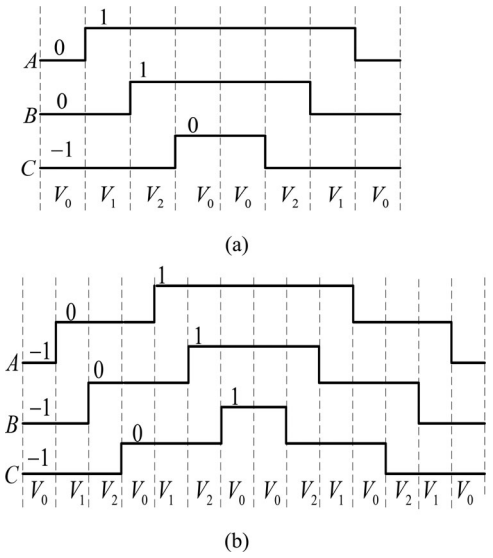

Fig. 2. (a) Eight segment SVM switching sequence in three-level inverters. (b) Fourteen segment SVM switching sequence in three-level inverters.

TABLE I
SSVMS WITCHING SEQUENCES

Triangle	Total number of switching states	Segments
A	7	6, 8, 10, 12, 14
C	5	6, 8, 10
B and D	4	6, 8

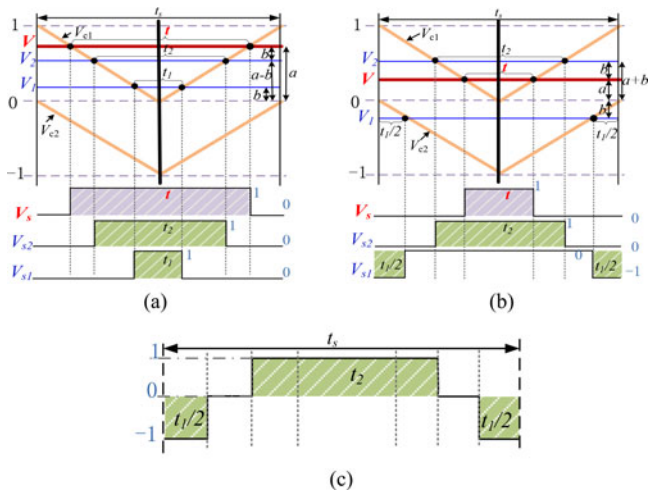

Fig. 3. Two decomposing cases of modulation wave and the combined pulse. (a) First decomposition case. (b) Second decomposition case. (c) Combined pulse synthesized by the two submodulation waves.

CBPWM with the same effect as SVM [2], [8], [9], and it can be easy realized.

Fig. 1(a) shows the main circuit of three-phase neutral-point-clamped (NPC) voltage source inverter (VSI). The space vector diagram of this inverter is showed in Fig. 1(b). Relevant detail conception and operation steps can refer to the literature [10]–[12].

TABLE II
AMPLITUDE VALUE OF MODULATION WAVES IN TWO DECOMPOSITION CASES

Modulation wave	The first case	The second case
$\boldsymbol{V}$	a	a
$\boldsymbol{V}_1$	b	−b
$\boldsymbol{V}_2$	a − b	a + b

Redundant state of the space vector is one of the most remarkable feature of SVM. [13] has indicated that different distribution of zero vectors or the placement of the small vectors can generate totally different results, the balance of neutral point voltage can be achieved by adjusting the redundant states duration proportion. In addition, [14]–[17] have shown that arranging the redundant states of zero vectors or small vectors properly can have many benefits, such as du/dt reduction, low switching frequency and voltage stress, the balance of the neutral point voltage in NPC, and the current harmonic distortion. Center-pulse double-edged seven segments SVM sequence, sometimes also called eight segments sequencesis depicted in Fig. 2(a). Defined this conventional SVM sequences as CSVMS. There are also some SSVMS, which include more than eight segments, named as SSVMS in this paper.

SSVMS is a special PWM sequences, which is more than eight segments, e.g., 10, 12, or 14, widely used in the practical PWM modulation process. Numerous researchers have verified that SSVMS can optimize the control effect of the three-level NPC inverter. Lin *et al.* [18] research the issues of neutral-point voltage control from point of view of SSVMS in detail. A simple neutral-point voltage balancing control method for three-level NPC inverters is proposed. Based on the SSVMS, the small vectors that will move the neutral point voltage in the direction opposite from the direction of unbalance can be selected. The experiment results illustrate that the performance of the proposed approach is satisfactory. In [19], the SVM of the three-level NPC inverter is analyzed. Based on the SSVMS, the PWM sequences are mended in order to reduce the total harmonics distortion of inverter output. Due to many switching state redundancies, the selection and arrangement of the SSVMS for the three-level NPC inverter still seem to be ambiguous and complicated. In [20], a general method for the selection of modulation sequences is established, which is suitable for the three-level NPC inverter. The advantages of the SSVMS are optimizing the output voltage and current and balancing the dc power, reducing the THD, controlling the neutral point voltage, and other respects in NPC [18], [19]. The disadvantage of the SSVMS is more complicated and more power loss than the CSVMS [20].

Taking Section I as an example, the four triangles in this section are A, B, C, and D as shown in Fig. 1(c). As mentioned in [21], the maximum sequences in triangle A is achieved by making use of all these seven states: (−1 −1 −1)→(0 −1 −1)→(0 0 −1)→(0 0 0)→(1 0 0)→(1 1 0)→(1 1 1). Thus, the number of segments of this longest switching

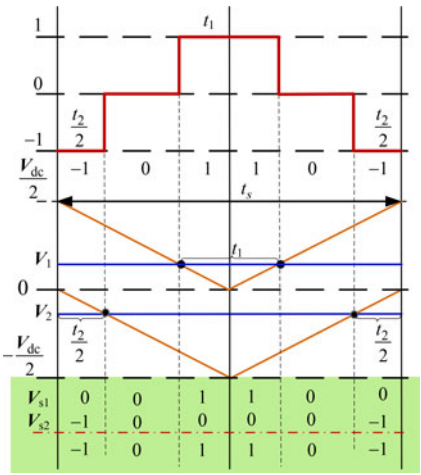

Fig. 4. Way to obtain the submodulation waves.

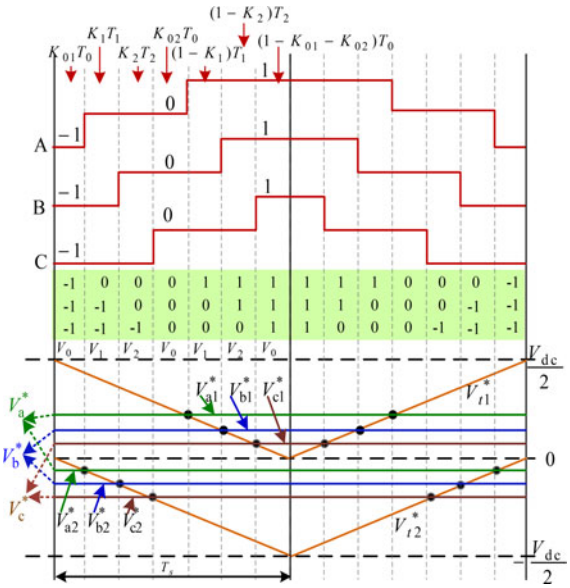

Fig. 5. Relationship between full-switching SSVMS and carrier-based PWM.

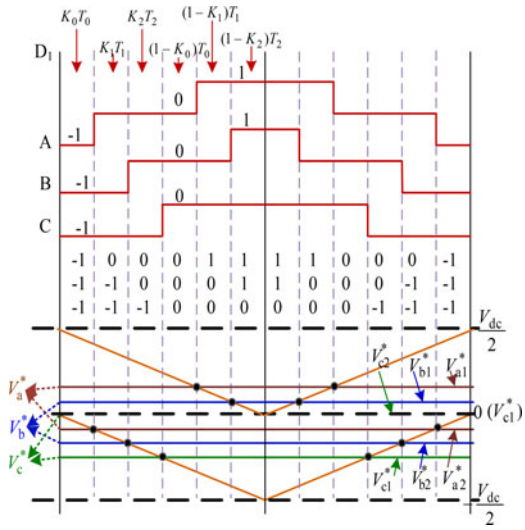

Fig. 6. Relationship between 12-segments SSVMS and carrier-based PWM.

TABLE III
MODULATION DECOMPOSING SYSTEM

Number of Segment	Sub-modulation waves (define : $V_{\max} \geq V_{\mathrm{mid}} \geq V_{\min}$)	Post-modulation Waves
8	if $V_x \geq 0\ x \in (\mathrm{a,b,c})$ then $V^*_{x1} = V_x + V_z,\ V^*_{x2} = 0;$ else $V^*_{x1} = 0,\ V^*_{x2} = V_x + V_z$	$V^*_x = V^*_{x1} + V^*_{x2} = V_x + V_z$
10	$V^*_{\max 1} = V_{\max} + V_z,\ V^*_{\max 2} = 0,$ $V^*_{\mathrm{mid}1} = V^*_{\mathrm{mid}1},\ V^*_{\mathrm{mid}2} = V^*_{\mathrm{mid}2},$ $V^*_{\min 1} = 0,\ V^*_{\min 2} = V_{\min} + V_z$	$V^*_{\max} = V_{\max} + V_z$ $V^*_{\mathrm{mid}} = V_{\mathrm{mid}} + V_z$ $V^*_{\min} = V_{\min} + V_z$
12	$V^*_{\max 1} = V^*_{\max 1},\ V^*_{\max 2} = V^*_{\max 2},$ $V^*_{\mathrm{mid}1} = V^*_{\mathrm{mid}1},\ V^*_{\mathrm{mid}2} = V^*_{\mathrm{mid}2},$ $V^*_{\min 1} = 0,\ V^*_{\min 2} = V_{\min} + V_z$	$V^*_{\max} = V_{\max} + V_z$ $V^*_{\mathrm{mid}} = V_{\mathrm{mid}} + V_z$ $V^*_{\min} = V_{\min} + V_z$
14	$V^*_{\max 1} = V^*_{\max 1},\ V^*_{\max 2} = V^*_{\max 2},$ $V^*_{\mathrm{mid}1} = V^*_{\mathrm{mid}1},\ V^*_{\mathrm{mid}2} = V^*_{\mathrm{mid}2},$ $V^*_{\min 1} = V^*_{\min 1},\ V^*_{\min 2} = V^*_{\min 2},$	$V^*_{\max} = V_{\max} + V_z$ $V^*_{\mathrm{mid}} = V_{\mathrm{mid}} + V_z$ $V^*_{\min} = V_{\min} + V_z$

sequence is $2 \times 7 = 14$ as shown in Fig. 2(b). Table I shows the number of all the optional SVM sequences in Section I.

The relationship between CSVMS and CBPWM has been studied adequately, the zero sequence has been acquired in many papers, but it does not get too much attention compared to the case of SSVMS and CBPWM. These preceding ways cannot calculate the zero component injection related to the SSVMS and the solution has not been seen in any literature.

The ultimate distinction between CSVMS and SSVMS is that each phase of the former can only output at most two voltage states like -1, 0 or 0, 1 as shown in Fig. 2(a), but each phase of the SSVMS can at most output three states as illustrated in Fig. 2(b). Some phase outputs three output states -1, 0, and 1 in one carrier cycle, which obviously cannot be obtained from the carrier-based PWM by using the same way as mentioned above. In [21], referring to the popular way of realizing multilevel SVM by decomposing the modulation wave into several two-level SVM, the author uses several carrier-based PWM modulation wave to synthesise the multilevel SVM successfully. However, the decomposition principle and the deduced implementation can't be used in the paper. In [10], a detail operation procedure and the resulting waveforms have been given for unifiing CSVMS and CBPWM with the injection of zero sequence, but this approach cannot apply to SSVMS as the reason explained above, hence a solution is needed.

In this paper, a decomposing technique has been revised so it can be applied to solve the aforementioned problems. Conception of "virtual modulation wave" (VMW) is proposed for the principle. Owing to this, then the accurate values of zero components, which is added into CBPWM to achieve SSVMS are obtained in the end; hence, the unified theory between CBPWM and SVM is improved in three-phase three-level inverters. The rest of this paper is structured as follows. Section II presents the decomposition principle and gives a strict theoretical proof for the principle of the new decomposition modulation wave method. An example of getting the relationship between CBPWM and SSVMS is shown in Section III. Amodulation

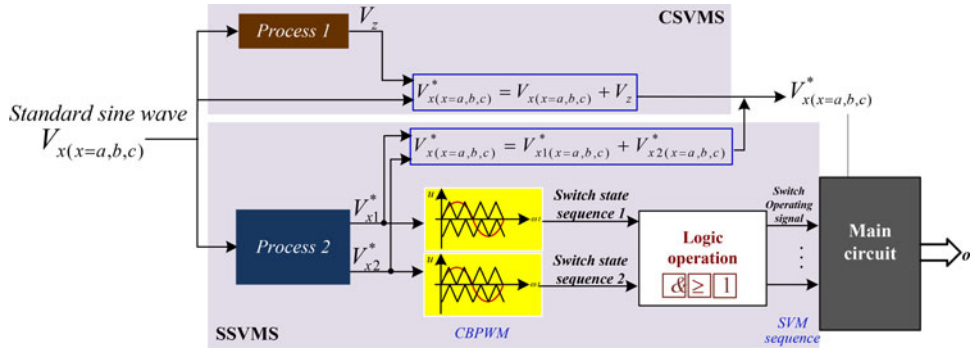

Fig. 7. Simple flowchat of CBPWM+Vz.

TABLE IV
SWITCHING STATE PATTERN OF TEN SEGMENTS SSVMS IN TRIANGLES D7–D12

Triangle in Fig. 1(b)	V_0	V_1	V_2	V_0	V_1	V_1	V_0	V_2	V_1	V_0
D7	0	0	1	1	1	1	1	1	0	0
	−1	0	0	0	1	1	0	0	0	−1
	−1	−1	−1	0	0	0	0	−1	−1	−1
D8	−1	0	0	0	1	1	0	0	0	−1
	0	0	1	1	1	1	1	1	0	0
	−1	−1	−1	0	0	0	0	−1	−1	−1
D9	−1	−1	−1	0	0	0	0	−1	−1	−1
	0	0	1	1	1	1	1	1	0	0
	−1	0	0	0	1	1	0	0	0	−1
D10	−1	−1	−1	0	0	0	0	−1	−1	−1
	−1	0	0	0	1	1	0	0	0	−1
	0	0	1	1	1	1	1	1	0	0
D11	−1	0	0	0	1	1	0	0	0	−1
	−1	−1	−1	0	0	0	0	−1	−1	−1
	0	0	1	1	1	1	1	1	0	0
D12	0	0	1	1	1	1	1	1	0	0
	−1	−1	−1	0	0	0	0	−1	−1	−1
	−1	0	0	0	1	1	0	0	0	−1
			$t_s/2$					$t_s/2$		

decomposition system and some rules during the procedure are also put forward in this section. The simulation and experimental waveforms are described in Section IV. Finally, the conclusions are given in Section V.

II. DECOMPOSITION PRINCIPLE

A. Modulation Wave Decomposition

In order to sovle the above mentioned problem, a modified decomposition that can generate three-level output states in one switching cycle is presented theoretically in this section. Generally, the decomposition of every modulation wave into two submodulation waves is done by the rule that the sum of these two submodulation wave values must be equivalent to the value of the original modulation wave, thus this results in 2 cases. Both of the cases are shown in Fig. 3(a) and (b), and all the amplitude values included in the figure are shown in Table II.

The original modulation wave is $\boldsymbol{V}$ and its amplitude is larger than the two carrier waves during time t. $\boldsymbol{V}_1$ and $\boldsymbol{V}_2$ are two submodulation waves. Two triangle carrier waves are $\boldsymbol{V}_{c1}$ and $\boldsymbol{V}_{c2}$ and their amplitudes are smaller than the two submodulation waves amplitudes $\boldsymbol{V}_1$ and $\boldsymbol{V}_2$ during the time t_1 and t_2, respectively. The carrier cycle is $\boldsymbol{V}_s$. The decomposition rule is based on a simple summation, i.e., $\boldsymbol{V} = \boldsymbol{V}_1 + \boldsymbol{V}_2$.

From one aspect it can be verified that the sum of intersection areas of the two submodulation waves ($\boldsymbol{V}_1$ and $\boldsymbol{V}_2$) with the zero axis is equal to the intersection area of the original modulation wave $\boldsymbol{V}$ with the zero axis, mathematically shown as $at_s = (a-b)t_s + bt_s = (a+b)t_s + (-b)t_s$.

From another aspect, the modulation wave is the sum of the two submodulation waves also been proved by the "Equal Area Theorem," which is depicted as follows:

Case 1 [see Fig. 3(a)]: $t_1 + t_2 = \dfrac{b}{a}t + \dfrac{a-b}{a}t = t$

Case 2 [see Fig. 3(b)]: $t_1 + t_2 = \dfrac{-b}{a}t + \dfrac{a+b}{a}t = t.$

Therefore, both of above mentioned proofs indicate that the sum of the two submodulation waves functioning equivalently to the original one. As illustrated in Fig. 3(c), a combined three-level switching sequence can be obtained more easily by synthesizing two submodulation wave in the second case shown in Fig. 3(b) than the first case. The synthesizing rule is that the combined pulse in Fig. 3(c) should have the exact same output performance as the modulated pulse of $\boldsymbol{V}$ in Fig. 3(b). $\boldsymbol{V}$ is called as postmodulation wave. Defining the CBPWM modulation wave of this three-level switching sequenceas "VMW". According to the carrier-based PWM characteristics, the VMW exists theoretically but not exist practically; therefore, the way to get three levels in one carrier cycle is found, and the new concept of the VMW is put forward that can be used for the theoretical analysis in the next paragraph.

B. Acquiring Submodulation Wave

As for SSVMS, to achieve the unified theory, the most important part is to get zero sequence of CBPWM going through the derivation reversely can help to get the corresponding two submodulation waves and the logical relationships. This process is presented as follows.

Taking a single-phase three-level SVM sequence (−1→0→1→1→0→−1) in Fig. 4 as an example. The three-level SVM sequence can be divided into two two-level SVM

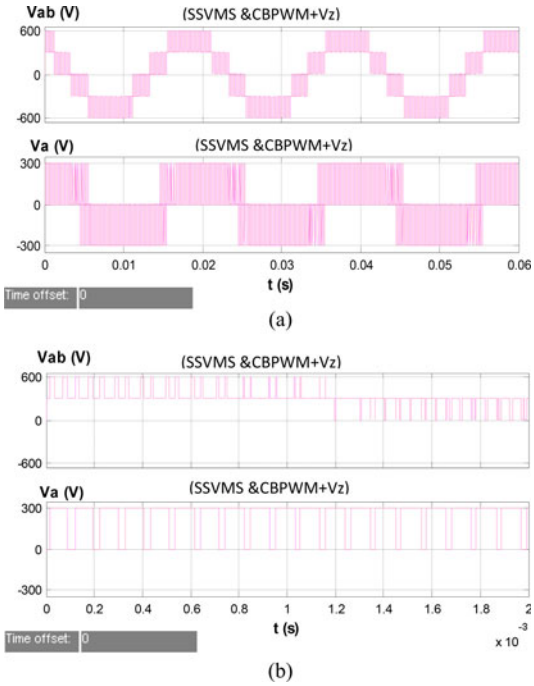

Fig. 8. (a)Waveforms of line voltage output V_{ab} and phase voltage output V_{a} when $m = 0.7$. (b) Zoomed capture of (a).

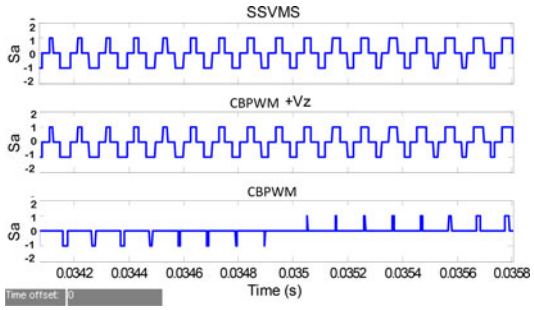

Fig. 9. Switching state comparison of phase *A*.

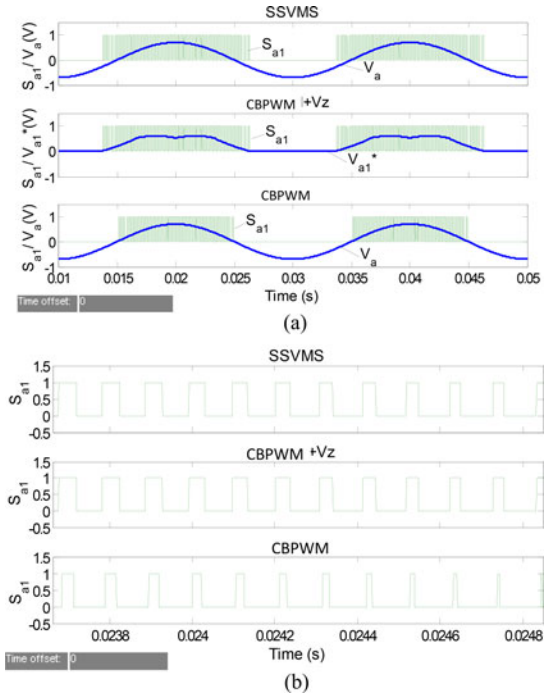

Fig. 10. (a) Switching pulse comparison of S_{a1}. (b) Switching pulse comparison of S_{a1} (zoom in).

TABLE V
MODULATION INDEX AND ITS PASSING AREA

$m = V_{\mathrm{ref}}/U_{\mathrm{dc}}/2$	Passed through triangle area	Modulation area	Segments included
0.5	A	inner	Case 1: eight segments Case 2: 12 segments Case 2: 14 segments
0.7	A and C	middle and outer	eight segments with ten segments
1	B, C and D	middle and outer	eight segments with ten segments

sequences: (0→0→1→1→0→0) and (−1→0→0→0→0→-1). Using those two CBPWM modulation waves V_1 and V_2, the two CSVMS can be easily achived by CBPWM, respectively.

In order to get the equivalently CBPWM postmodulation wave to three-level SVM sequence, getting the two CBPWM submodulation waves of the two two-level SVM sequences is foremost. According to those two two-level SVM sequences in Fig. 4, the value of two CBPWM submodulation waves V_1 and V_2 can be obtained.The logical process between the CSVMS wave and these two submodulated SVM wave in every sampling period as describes in next paragraph, making sure the logical calculated result of these two submodulated SVM is exactly the same as the original three-level SVM sequence.

The purpose of finding the logical relationship is that the total output performance of these two modulated square waves should be equivalent to that of the original SVM sequence. The summation logics are expressed as $-1+0=-1; 0+0=0; 1+0=1$. If the three output states are expressed with 2, 1, 0 instead of -1, 0, 1, then the corresponding logical relationshipsare will be changed to be $0+1=0; 1+1=1; 2+1=2$. Owing to this logic, the three-level output can be produced by combing the outputs of two submodulation waves.

III. UNIFIED THEORY BETWEEN CBPWM AND SVM

A. Theoretical Derivation of a 14-Segment SVM Sequence

Taking the full-SVM switching sequence, for example, which is shown in Fig. 5. Different switching state intervals are marked in the diagram, because of the symmetrical characteristics, the analysis can be concentrated on the half carrier period ($\boldsymbol{T}_{\mathrm{s}} = \boldsymbol{t}_{\mathrm{s}}/2$) only. T_0, T_1, and T_2 are the half duration of V_0, V_1, and V_2 in one switching period, respectively. The distribution

coefficients $K_{01}, K_{02}, K_0, K_1, K_2$ designate the percentage of every redundant switching state that corresponds to the same space vector in a half carrier period T_s. $V_{\rm a}^*$, $V_{\rm b}^*$, $V_{\rm c}^*$ are the postmodulation waves of each phase,using the decomposition method of modulation wave, submodulation waves of them V_{x1}^*, V_{x2}^* $(x = {\rm a}, {\rm b}, {\rm c})$ can be acquired, the V_{t1}^*, V_{t2}^* are the carrier waves. The relationship derivation can be made out as follows.

According to the principle of volt–second balance

$$\begin{cases} [(1-K_1)T_1 + K_1T_1]V_{\rm dc}/2 = T_sV_{\rm ab} \\ [(1-K_2)T_2 + K_2T_2]V_{\rm dc}/2 = T_sV_{\rm bc}. \end{cases} \tag{1}$$

Therefore

$$\begin{cases} T_0 = T_s\{1 - [V_{\rm ac}/(V_{\rm dc}/2)]\} \\ T_1 = T_sV_{\rm ab}/(V_{\rm dc}/2) \\ T_2 = T_sV_{\rm bc}/(V_{\rm dc}/2). \end{cases} \tag{2}$$

According to the Fig. 5, every submodulation wave can be written as

$$\begin{cases} V_{\rm a1}^* = \dfrac{(1-K_{01}-K_{02})T_0 + (1-K_2)T_2 + (1-K_1)T_1}{T_s}\dfrac{V_{\rm dc}}{2} \\ V_{\rm a2}^* = \dfrac{K_{01}T_0}{T_s}\left(-\dfrac{V_{\rm dc}}{2}\right) \\ V_{\rm b1}^* = \dfrac{(1-K_{01}-K_{02})T_0 + (1-K_2)T_2}{T_s}\dfrac{V_{\rm dc}}{2} \\ V_{\rm b2}^* = \dfrac{K_1T_1 + K_{01}T_0}{T_s}\left(-\dfrac{V_{\rm dc}}{2}\right) \\ V_{\rm c1}^* = \dfrac{(1-K_{01}-K_{02})T_0}{T_s}\dfrac{V_{\rm dc}}{2} \\ V_{\rm c2}^* = \dfrac{K_2T_2 + K_1T_1 + K_{01}T_0}{T_s}\left(-\dfrac{V_{\rm dc}}{2}\right). \end{cases} \tag{3}$$

Substituting (2) into (3), submodulation waves V_{x1}^*, V_{x2}^* $(x = {\rm a}, {\rm b}, {\rm c})$ can be obtained by

$$\begin{cases} V_{\rm a1}^* = (K_{01}+K_{02}-K_1)V_{\rm a} + (K_1-K_2)V_{\rm b} + \\ \qquad (K_2-K_{01}-K_{02})V_{\rm c} + (1-K_{01}-K_{02})V_{\rm dc}/2 \\ V_{\rm a2}^* = K_{01}V_{\rm a} - K_{01}V_{\rm c} - K_{01}V_{\rm dc}/2 \\ V_{\rm b1}^* = (K_{01}+K_{02}-1)V_{\rm a} + (1-K_2)V_{\rm b} + \\ \qquad (K_2-K_{01}-K_{02})V_{\rm c} + (1-K_{01}-K_{02})V_{\rm dc}/2 \\ V_{\rm b2}^* = (K_{01}-K_1)V_{\rm a} + K_1V_{\rm b} - K_{01}V_{\rm c} - K_{01}V_{\rm dc}/2 \\ V_{\rm c1}^* = (K_{01}+K_{02}-1)V_{\rm a} + (1-K_{01}-K_{02})V_{\rm c} + \\ \qquad (1-K_{01}-K_{02})V_{\rm dc}/2 \\ V_{\rm c2}^* = (K_{01}-K_1)V_{\rm a} + (K_1-K_2)V_{\rm b} + \\ \qquad (K_2-K_{01})V_{\rm c} - K_{01}V_{\rm dc}/2. \end{cases} \tag{4}$$

According to $V_x^* = V_{x1}^* + V_{x2}^* (x = {\rm a}, {\rm b}, {\rm c})$, three postmodulation waves are

$$\begin{cases} V_{\rm a}^* = V_{\rm a} + V_{\rm z} \\ V_{\rm b}^* = V_{\rm b} + V_{\rm z} \\ V_{\rm c}^* = V_{\rm c} + V_{\rm z} \\ V_{\rm z} = -(K_1+1-2K_{01}-K_{02})V_{\rm a} + (K_1-K_2)V_{\rm b} + \\ \qquad (K_2-2K_{01}-K_{02})V_{\rm c} + (1-2K_{01}-K_{02})V_{\rm dc}/2. \end{cases} \tag{5}$$

Note that

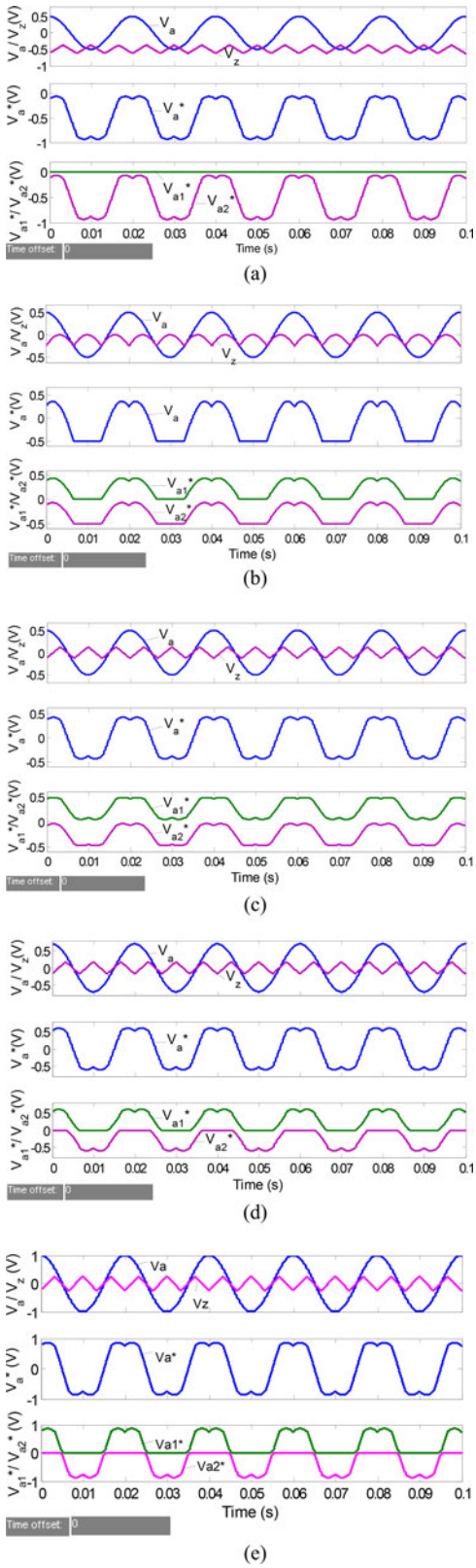

Fig. 11. (a) $m = 0.5$, $V_{\rm ref}$ passing throng inner modulation area with eight segments SVM. (b) $m = 0.5$, $V_{\rm ref}$ passing throng inner modulation area only including 12 segments SSVMS. (c) $m = 0.5$, $V_{\rm ref}$ passing throng Inner modulation area only including 14 segments SSVMS. (d) $m = 0.7$, $V_{\rm ref}$ passing throng middle and outer modulation area including eight and ten segments SSVMS. (e) $m = 1$, $V_{\rm ref}$ passing throng middle and outer modulation area including eight and ten segments SSVMS.

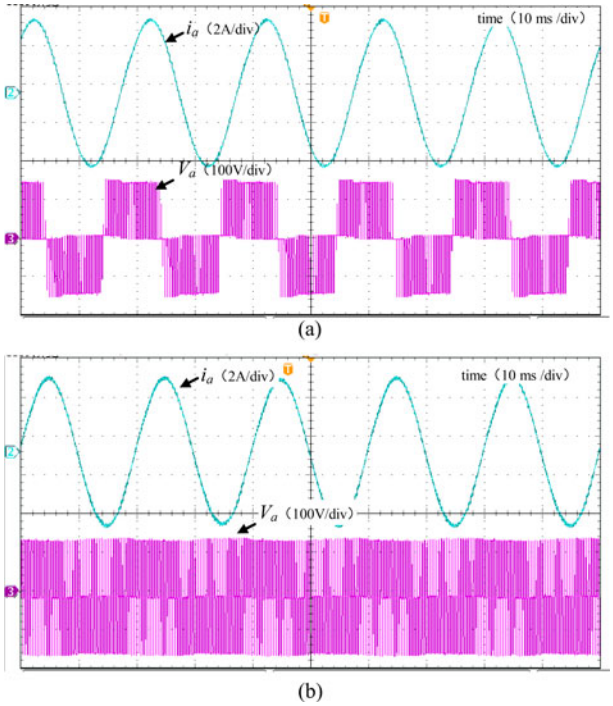

Fig. 12. $m = 0.3$, a comparison of phase voltage, and load current between CSVMS and SSVMS. (a) Eight segments sequence CSVMS method. (b). Fourteen segments sequence SSVMS method.

TABLE VI
COMPARISON OF CSVMS AND SSVMS

	segments	THD	switching commutation numbers in three phase	switching frequency
CSVMS	8	2.6%	12	2.4 kHz
SSVMS	14	1.7%	24	2.4 kHz

$V_{\mathrm{a}}, V_{\mathrm{b}}, V_{\mathrm{c}}$ are three standard sine modulation waves without adding anything else, named premodulation waves.

$V_{\mathrm{a}}^*, V_{\mathrm{b}}^*, V_{\mathrm{c}}^*$ are three modulation waves related to the SSVMS, named postmodulation waves.

V_z is zero sequence component.

Observing the above equations, it can be seen that $V_x^* = V_x + V_z (x = \mathrm{a}, \mathrm{b}, \mathrm{c})$. Hence, it reach the same conclusion as in CSVMS that the three-phase CBPWM modulation wave with zero component injection equals the SSVMS modulation wave.

B. Modulation Decomposition System

From the above, the following conclusions can be made:

1) the SVM sequence including three output states need two submodulation waves;
2) the SVM sequence with two output states only has one modulation wave, which is same as that of CSVMS;
3) the 14 segment sequence is the extreme case, in which each of three phases has two submodulation waves. The eight segment sequence is the least case in which each of three phases only has one submodulation wave. Ten and 12 segment sequences lay between the extreme cases.

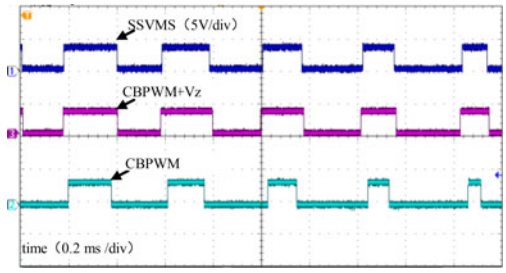

Fig. 13. Experiment waveforms of three switching pulse comparison.

In order to unify the derivation process for the sequence, which does not have two submodulation waves, consider one of the two submodulation waves is a zero amplitude wave, and another one is the original modulation wave. Take a 12 segments SVM sequences, as an example, as showed in Fig. 6. The ten segments sequences can also be obtained by the same calculation steps.

By strict derivation, the postmodulation wave of three phases and the added zero sequence component are

$$\begin{cases} V_{\mathrm{a}}^* = V_{\mathrm{a}} + V_{\mathrm{z}} \\ V_{\mathrm{b}}^* = V_{\mathrm{b}} + V_{\mathrm{z}} \\ V_{\mathrm{c}}^* = V_{\mathrm{c}} + V_{\mathrm{z}} \\ V_{\mathrm{z}} = (K_0 - K_1)V_{\mathrm{a}} + (K_1 - K_2)V_{\mathrm{b}} + \\ \qquad (-K_0 + K_2 - 1)V_{\mathrm{c}} - K_0 \dfrac{V_{\mathrm{dc}}}{2}. \end{cases} \tag{6}$$

Also, the amplitudes of $V_{x1}^* = V_{x2}^* (x = \mathrm{a}, \mathrm{b}, \mathrm{c})$ are

$$\begin{cases} V_{\mathrm{a}1}^* = (1 - K_1)V_{\mathrm{a}} + (K_1 - K_2)V_{\mathrm{b}} + (K_2 - 1)V_{\mathrm{c}} \\ V_{\mathrm{a}2}^* = K_0 V_{\mathrm{a}} - K_0 V_{\mathrm{c}} - K_0 \dfrac{V_{\mathrm{dc}}}{2} \\ V_{\mathrm{b}1}^* = (1 - K_2)V_{\mathrm{b}} - (1 - K_2)V_{\mathrm{c}} \\ V_{\mathrm{b}2}^* = (K_0 - K_1)V_{\mathrm{a}} + K_1 V_{\mathrm{b}} - K_0 V_{\mathrm{c}} - K_0 \dfrac{V_{\mathrm{dc}}}{2} \\ V_{\mathrm{c}1}^* = (K_0 - K_1)V_{\mathrm{a}} + (K_1 - K_2)V_{\mathrm{b}} + \\ \qquad (-K_0 + K_2)V_{\mathrm{c}} - K_0 \dfrac{V_{\mathrm{dc}}}{2} \\ V_{\mathrm{c}2}^* = 0. \end{cases} \tag{7}$$

For SVM with different segments sequence, the whole modulation decomposition system is shown in Table III. Before decomposition, the first step is to detect the value of three phases in each sampling period and grade to $V_{\max}, V_{\mathrm{mid}}, V_{\min}$, which are the maximum, middle, and minimum value of phase voltage, respectively, and V_{m1}, V_{m2} $(m = \max, \mathrm{mid}, \min)$ are their two submodulation waves, respectively. The related data during the decomposition method is shown in the Table III. The procedure of CBPWM+Vz is shown in the process schematic Fig. 7 below. *Process 1* and *2* stand for the way by which V_z and V_{x1}^*, V_{x2}^* can be obtained, respectively, from the premodulation waves $V_x (x = \mathrm{a}, \mathrm{b}, \mathrm{c})$. Take the aforementioned equations as an example, the fourth equation in both (5) and (6) can on behalf of *Process 1*; (4) and (7) can on behalf of *Process 2*.

From the (5) and (6), the inherent relationship between SSVMS and CBPWM has been proved. More importantly, the zero component (V_z) has been obtained. The conclusion develops the unified theory between three-level SVM and

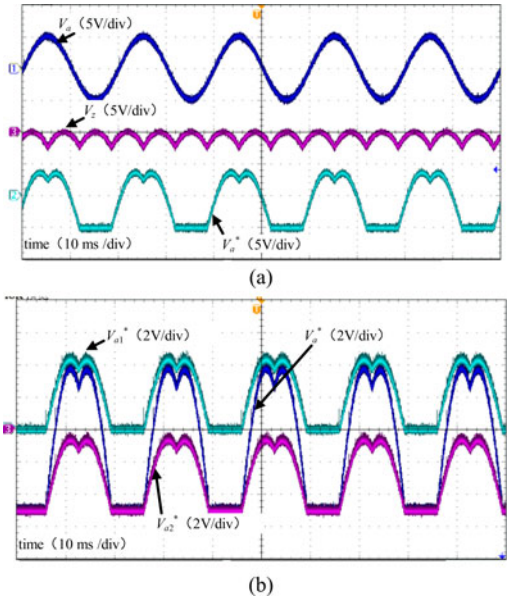

Fig. 14. $m = 0.5$, V_{ref} passing throng Inner modulation area with 12 segments SSVMS. (a) Experiment waveforms of V_{a}, V_z, and V_{a}^*. (b) Experiment waveforms of $V_{\mathrm{a}1}^*$, V_{a}^*, and $V_{\mathrm{a}2}^*$.

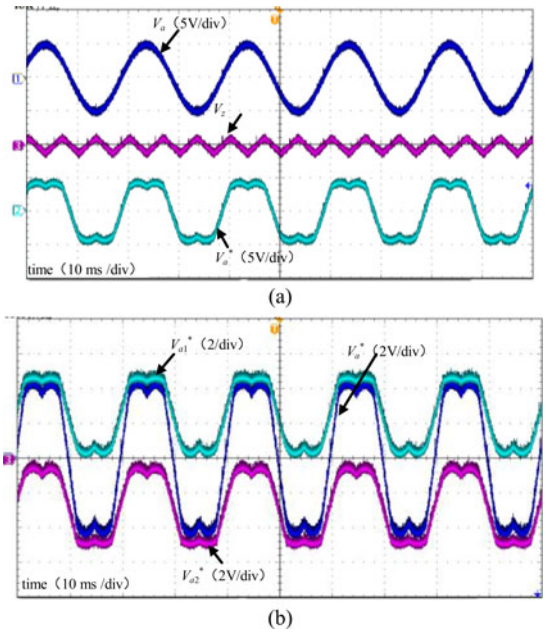

Fig. 15. $m = 0.5$, V_{ref} passing throng inner modulation area with 14 segments SSVMS. (a) Experiment waveforms of V_{a}, V_z, and V_{a}^*. (b) Experiment waveforms of $V_{\mathrm{a}1}^*$, V_{a}^*, and $V_{\mathrm{a}2}^*$.

the carrier-based PWM. It also affirms the feasibility of the decomposition modulation wave method. The distribution coefficients K_{01}, K_{02}, K_0, K_1, and K_2 are flexible. Altered distribution coefficients can produce different SSVMS and also different V_z. The submodulation waves can be calculated easily if the coefficients are given, which contribute to realizing SSVMS by CBPWM in practice.

Additionally, all the deduction above can be applied to any other area of the entire space vector diagram.

IV. Simulation and Experimental Results

A. Simulation

The three-level NPC VSI in Fig. 1 has been simulated using MATLAB. The expression of modulation index is $m = V_{\mathrm{ref}}/\frac{U_{\mathrm{dc}}}{2}$. All the redundant switching statesis assumed to share equivalent interval time. The dc voltage is set as 600 V with resistive load. Switching frequency is 10k Hz, and the standard modulation wave frequency is 50 Hz. SSVMS design is the first task for simlation or experimen. For simplicity, all the SSVMS studied in the simulation and experiments distribute their redundant states averagely, namely $K_{01} = K_{02} = 1/3$, $K_0 = K_1 = K_2 = 1/2$. As the switching pattern for 14 and 12 segemtns SSVMS have already been listed in Figs. 5 and 6, Table IV shows the switching state pattern including ten segments SSVMS in triangles D7– D12 clearly. After the SSVMS determination, the zero component (V_z) and every submodulation wave V_{x1}^*, V_{x2}^* ($x = \mathrm{a}, \mathrm{b}, \mathrm{c}$) can be acquired easily by using the modulation wave decomposing approach which presented in this paper.

The main purpose of the simulation and experiment is to verify whether the two modulation strategies, i.e., CBPWM with zero component injection (CBPWM+Vz) and SSVMS have the exact same effect. To see this obviously, CBPWM without the zero injectionis considered as a comparison. The output voltage waveforms of the NPC VSI modulated by SVM and CBPWM+Vz when $m = 0.7$ are shown in Fig. 8. V_{ab} is the line to line voltage between phase *A* and *B* and V_a is the phase *A* voltage. Fig. 8(b) is zoomed capture of Fig. 8(a), which displays the overlap more clearly. So the output voltages of SSVMS and CBPWM+Vz are the same ones. The same condition can be seen in phase voltage V_{a}.

Fig. 8 shows the waveforms of line voltage output V_{ab} and phase voltage output V_{a} modulated by SVM and CBPWM+Vz when $m = 0.7$.

Fig. 9 shows the switching state of phase *A* under three modulation strategies. At each moment, the switching state of CBPWM+Vz behaves the same as SSVMS but completely differs from CBPWM. Similar behavior can be noticed when observing the switching pulse of a certain switch, as shown in Fig. 10(a) and (b). Fig. 10(a) shows the switching pulse of S_{a1} under three modulation strategies. Fig. 10(b) is the zoomed figure of Fig. 10(a).These results verify the correctness that the zero sequence component of CBPWM+Vz is correct and have the same effect as SSVMS. All above conclusions from Figs. 8–10 keep valid for different *m* cases and SSVMS.

Additionally, the cases of $m = 0.5, 0.7$ and 1 are choosed to test in the simulation and expenriment process. Take Table I and Fig. 1(c) into accout, the connection between modulatoin index and sequence segments are listed in Table V. Different wave forms combination in CBPWM+Vz corresponding to different SSVMS are shown from Fig. 11(a) to (e). All the wave values are between -1 and 1 due to the normalization.

Note that:

V_{a}—is the pre-modulation wave of phase *A*;

V_z—is the zero sequence component wave;

V_a^*—is the postmodulation wave of phase *A*;

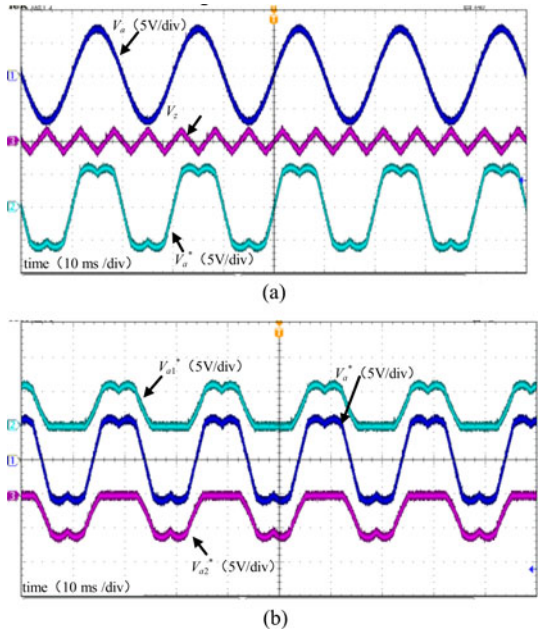

Fig. 16. $m = 0.7$, $V_{\rm ref}$ passing throng middle and outer modulation area with eight and ten segments SSVMS. (a) Experiment waveforms of $V_{\rm a}$, V_z, and $V_{\rm a}^*$. (b) Experiment waveforms of $V_{\rm a1}^*$, $V_{\rm a}^*$, and $V_{\rm a2}^*$.

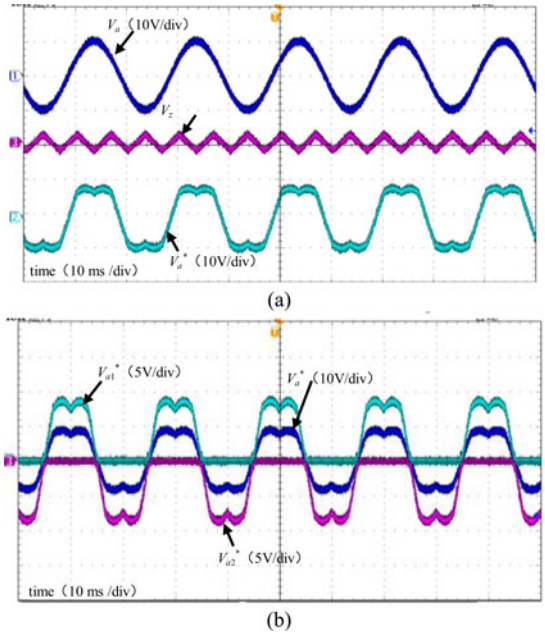

Fig. 17. $m = 1$, $V_{\rm ref}$ passing throng middle and outer modulation area with eight and ten segments SSVMS. (a) Experiment waveforms of $V_{\rm a}$, V_z, and $V_{\rm a}^*$. (b) Experiment waveforms of $V_{\rm a1}^*$, $V_{\rm a}^*$, and $V_{\rm a2}^*$.

V_{a1}, V_{a2}—is two submodulation waves;one is larger than or equal to 0; the other is lower than or equal to 0.

The above figures indicate that different SSVMS and different modulation index cause different ***V***z injected into CBPWM. But all of them satisfy the eqution $V_x^* = V_{x1}^* + V_{x2}^* (x = \mathrm{a}, \mathrm{b}, \mathrm{c})$, which verifies the rightness of decomposition method of modulation wave.

B. Experiments

An experiment platform used for verifying the proposed unified theory has been set up. Retated experiment parameters are listed as following: DSP (F28335) of TI Company, FPAG (Cyclone II series EP2C35F484C8) of Altera Company, Dc-bus voltage Ud = 120 V, Cdc1 = Cdc2 = 4700 μF, Rload = 5.3 Ω, load = 5.4 mH, and switching frequency of the inverter is chosen to be 2.4 kHz. The comparison experiments to illustrate the pros and cons for using such SSVMS has been done at first. When $m = 0.3$, as can be seen from Fig. 12 where phase voltage V_a, and load current i_a are shown for two PWM techniques in the three-level NPC inverter. Fig. 12(a) is CSVMS method which outputs 8 segments sequence and two voltage level in each switching cycle. Fig. 12(b) is SSVMS method which outputs 14 segments and three voltage level in each switching cycle. By analyzing the THD of load current, the 14 segments SSVMS is 1.7%; that is much better than eight segments CSVMS which is 2.6%. As shown in Table VI, when the switching frequencies are the same, the switching commutation numbers of SSVMS is double than CSVMS in one switching cycle, which obviously means more power loss. In a summery, it can be seen that the advantages of SSVMS are optimizing the output current and reducing the THD. The disadvantage of the SSVMS is that the switching commutation is much more than CSVMS, the power loss is bigger than the CSVMS.

Fig. 13 shows the experimental results for switching pulses of three strategies. Comparing the results, the switching pulses of $S_{\rm a1}$ under SSVMS and CBPWM+Vz have the identical waveforms. Whats more, Figs. 14–17 shows different modulation waveforms of CBPWM+Vz corresponding 8,10,12, and14 segment SSVMS when $m = 0.5, 0.7$ and 1, respectively, which reflect completely similar as the simulation results depicted in Fig. 12(b)–(e). Therefore both simulation and experiment can achieve the same conculsion that SSVMS function equivalently to CBPWM with corresponding zero component injection.

V. Conclusion

This paper improves the unified theory between CBPWM and SVM in three phase three-level VSI. It deeply concentrates on acquisition of the zero sequence component and the relationship between CBPWM and SSVMS which has not been proposed before. The strict theory, simulation and experimental results verify the proposed idea and all the results are found to be correct and similar. Moreover the new idea of VMW has also been proposed which is specially used to correlate carrier-based PWM with SSVMS. In addition the procedure of getting the submodulation waves and their logical relationship has been put forward. Finally, the conclusion that the SSVMS can also be equivalently realized by the CBPWM with an accurate zero component addition is demonstrated and this decomposing method can be extended to verifythe unified theory of CBPWM and SVM with any other segments sequences.

REFERENCES

[1] K. L. Zhou and D. W. Wang, "Relationship between space-vector modulation and three-phase carrier-based PWM: A comprehensive analysis three-phase inverters," *IEEE Trans. Ind. Electron.*, vol. 49, no. 1, pp. 186–196, Feb. 2002.

[2] K. Sri Gowri, T. Brahmananda Reddy, and C. Sai Babu, "A novel high performance generalized discontinuous PWM algorithm for reduced current ripple and switching losses using imaginary switching times," in *Proc. IEEE TENCON Region 10 Conf.,* Hyderabad, India, Nov. 2008, pp. 1–6.

[3] R. Burgos, R. X. Lai, Y. Q. Pei, F. Wang, D. Boroyevich, and J. Pou, "Space vector modulator for vienna-type rectifiers based on the equivalence between two- and three-level converters: A carrier-based implementation," *IEEE Trans. Power Electron.*, vol. 23, no. 4, pp. 1888–1898, Jul. 2008.

[4] A. M. Hava and N. Onur Cetin, "A generalized scalar PWM approach with easy implementation features for three-phase, three-wire voltage-source inverters," *IEEE Trans. Power Electron.*, vol. 26, no. 5, pp. 1385–1395, May 2011.

[5] S. Jian and L. Yun Wei, "A space-vector modulation method for common-mode voltage reduction in current-source converters," *IEEE Trans. Power Electron.*, vol. 29, no. 1, pp. 374–385, Jan. 2014.

[6] O. Dordevic, E. Levi, and M. Jones, "A vector space decomposition based space vector PWM algorithm for a three-level seven-phase voltage source inverter," *IEEE Trans. Power Electron.*, vol. 28, no. 2, pp. 637–649, Feb. 2013.

[7] A. Iqbal and S. Moinuddin, "Comprehensive relationship between carrier-based PWM and space vector PWM in a five-phase VSI," *IEEE Trans. Power Electron.*, vol. 24, no. 10, pp. 2379–2390, Oct. 2009.

[8] W. X. Song, G. C. Chen, X. Y. Ding, and M. T. Shu, "Research on neutral-point balancing control for three-level NPC inverter based on correlation between carrier-based PWM and SVPWM," in *Proc. IEEE 5th Power Electron. Motion Control Conf.*, Shanghai, China, 14–16 Aug., 2006, vol. 3, pp. 1–6.

[9] J. Pou, J. Zaragoza, S. Ceballos, M. Saeedifard, and D. Boroyevich, "A carrier-based PWM strategy with zero-sequence voltage injection for a three-level neutral-point-clamped converter," *IEEE Trans. Power Electron.*, vol. 27, no. 2, pp. 642–651, Feb. 2012.

[10] D. P. Cao, W. X. Song, H. Xi, G. C. Chen, and C. Chen, "Research on zero-sequence signal of space vector modulation for three-level neutral-point-clamped inverter based on vector diagram partition," in *Proc. IEEE 6th Int. Power Electron. Motion Control Conf.*, Wuhan, China, 17–20 May, 2009, pp. 1435–1439.

[11] N. V. Nho and M. J. Youn, "Comprehensive study on space-vector-PWM and carrier-based-PWM correlation in multilevel invertors," *IEE Proc. Electric Power Appl.*, vol. 153, pp. 149–158, Jan. 2006.

[12] C. Sourkounis and A. Al-Diab, "A comprehensive analysis and comparison between multilevel space-vector modulation and multilevel carrier-based PWM," in *Proc. 13th Power Electron. Motion Control Conf.*, Poznan, Poland, Sep. 2008, pp. 1710–1715.

[13] N. Celanovic and D. Boroyevich, "A comprehensive study of neutral-point voltage balancing problem in three-level neutral-point-clamped voltage source PWM inverters," *IEEE Trans. Power Electron.*, vol. 15, no. 2, pp. 242–249, Mar. 2000.

[14] S. Das and G. Narayanan, "Novel switching sequences for a space-vector-modulated three-level inverter," *IEEE Trans. Ind. Electron.*, vol. 59, no. 3, pp. 1477–1487, Mar. 2012.

[15] A. R. Beig and V. T. Ranganathan, "Influence of placement of small space vectors on the performance of PWM techniques for three level inverters," in *Proc. IEEE 29th Annu. Conf. Ind. Electron. Soc.*, Nov. 2003, vol. 3, pp. 2764–2770.

[16] V. T. Somasekhar, S. Srinivas, and K. K. Kumar, "Effect of zero-vector placement in a dual-inverter fed open-end winding induction-motor drive with a decoupled space-vector PWM strategy," *IEEE Trans. Ind. Electron.*, vol. 55, no. 6, pp. 2497–2505, Jun. 2008.

[17] Z. G. Yin, C. W. Liu, K. Wang, and Y. H. Li, "The arrangement of switching sequences in SVPWM for neutral-point-clamped converter," in *Proc. Int. Conf. Electr. Mach. Syst.*, Incheon, Korea, Oct. 2010, pp. 225–229.

[18] L. Lin, Y. P. Zou, Z. Wang, and H. Y. Jin, "A simple neutral-point voltage balancing control method for three-level NPC PWM VSI inverters," in *Proc. IEEE Int. Conf. Electr. Mach. Drives.*, San Antonio, TX, USA, May 2005, pp. 828–833.

[19] W. Tian, J. Zhang, and Z. Zhang, "Research on energy feedback based on SVPWM algorithm for three-level," in *Proc. Intell. Inf. Process. Trusted Comput. Int. Symp.*, Huanggang, China, Oct. 2010, pp. 110–113.

[20] M. Ke and F. Blaabjerg, "Unifying and generating of space vector modulation sequences for multilevel converter," in *Proc. IEEE 29th Annu. Appl. Power Electron. Conf. Expo.*, Mar. 2014, pp. 196–201.

[21] W. X. Yao, H. B. Hu, and Z. Y. Lu, "Comparisons of space-vector modulation and carrier-based modulation of multilevel inverter," *IEEE Trans. Power Electron.*, vol. 23, no. 1, pp. 45–51, Jan. 2008.

Juan Chen was born in Hunan Province, China, in 1988. She received the B.S. degree from the Central South University, Hunan, in 2010, and the M.S. degree from Xi'an Jiaotong University, Xi'an, China, in 2013.

She is currently working as an Engineer with New Energy Company. Her research interests include multilevel inverters, solar converter, power-quality control, and the application of power electronics in power systems.

Yingjie He (M'07) was born in Henan Province, China, in 1978. He received the B.S., M.S., and Ph.D. degrees from the Huazhong University of Science and Technology, Wuhan, China, in 1999, 2003, and 2007, respectively.

From May 2007 to May 2009, he was with the Power Electronics and Renewable Energy Center, Xi'an Jiaotong University, Xi'an, China, as a Postdoctoral Researcher, where he is currently an Associate Professor. His current research interests include power quality control, multilevel inverters, and the application of power electronics in power systems.

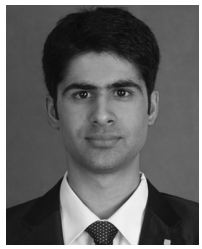

Saad Ul Hasan (S'09–M'14) was born in Pakistan in 1989. He has received the B.S degree from Bahria University, Islamabad, Pakistan, and the M.S degree from Xi'an Jiaotong University (XJTU), Xi'an, China.

From September 2011 to July 2013, he was with Power Electronics & Renewable Energy Research Center, as a Graduate Student with XJTU. He is currently working as a Lecturer at the Department of Electrical Engineering, Bahria University, Islamabad. His research interests include dc–dc converters, magnetics, and integration of renewable energy sources in distributed power systems.

Jinjun Liu (M'98–SM'10) was born in Hunan Province, China, in 1970. He received the B.S. and Ph.D. degrees from Xi'an Jiaotong University (XJTU), Xi'an, China, in 1992 and 1997, respectively.

In 1998, he led the founding of the XJTU/Rockwell Automation Laboratory. From December 1999 to February 2002, he was with the Center for Power Electronics Systems, Virginia Polytechnic Institute and State University, Blacksburg, VA, USA, as a Postdoctoral Research Scholar. In August 2002, he was promoted to the Full Professor and the Head of the Power Electronics and Renewable Energy Center, XJTU, where he is currently an Associate Dean at the School of Electrical Engineering. He has coauthored three books and published more than 100 technical papers. His current research interests include power quality control, renewable energy generation, utility applications of power electronics, and the modeling and control of power electronic systems. He was actively involved in the organization of several power electronic international conferences, including PESC, APEC, IPEC in Japan, ICPE in Korea, and IPEMC in China, where he served as a Committee Member, a Co-Chair, or a Session Chair.

Dr. Liu received several provincial or ministerial awards for scientific and career achievements. He also received the 2006 Delta Scholar Award. He served as the IEEE Power Electronics Society Region 10 Liaison for three years.